Electronic Supplementary Material (ESI) for Nanoscale.

Journal Name

ARTICLE

Electronic Supporting Information

Cis-platinum Pro-Drug-Attached $CuFeS_2$ Nanoplates for *In Vivo* Photothermal/Photoacoustic Imaging and Chemotherapy/Photothermal Therapy of Cancer

Binbin Ding[a,e], Chang Yu[a,f], Chunxia Li*[,b], Xiaoran Deng[a,f], Jianxun Ding[c], Ziyong Cheng[a], Bengang Xing[d], Ping'an Ma*[,a], Jun Lin*[,a]

[a] *State Key Laboratory of Rare Earth Resource Utilization, Changchun Institute of Applied Chemistry, Chinese Academy of Sciences, Changchun, 130022, China.*

[b] *Institute of Physical Chemistry, Zhejiang Normal University, Jinhua, Zhejiang, 321004, China.*

[c] *Key Laboratory of Polymer Ecomaterials, Changchun Institute of Applied Chemistry, Chinese Academy of Sciences, Changchun 130022, China.*

[d] *School of Physical & Mathematical Sciences, Nanyang Technological University, Singapore.*

[e] *University of Science and Technology of China, Hefei, 230026, China.*

[f] *University of Chinese Academy of Sciences, Beijing, 100049, China.*

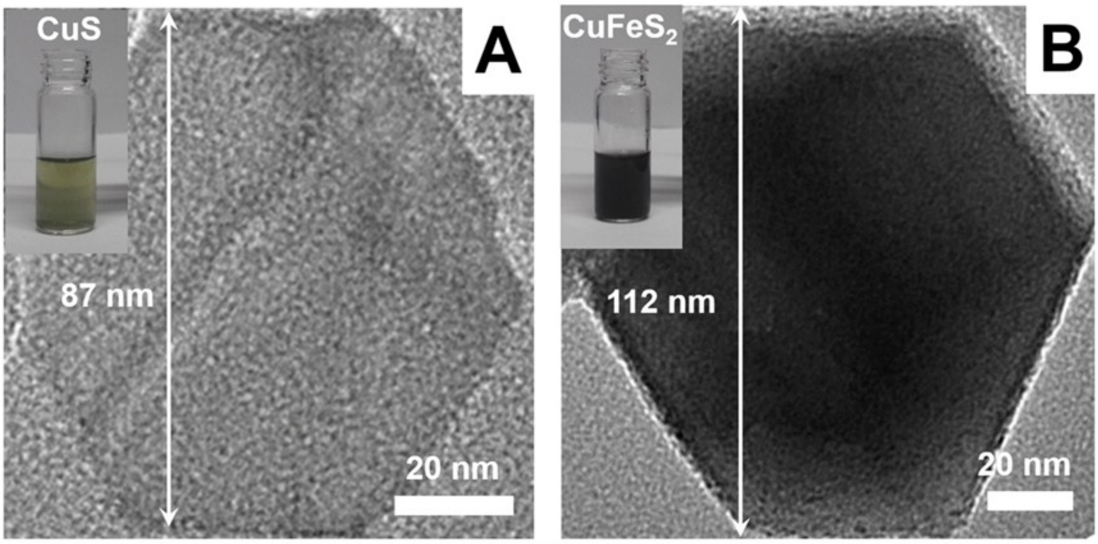

Figure S1. TEM images of OLE coated CuS NPs (A), $CuFeS_2$ NPs (B). Digital photographs of CuS NPs dispersed in toluene, $CuFeS_2$ NPs dispersed in toluene (inserts of A and B).

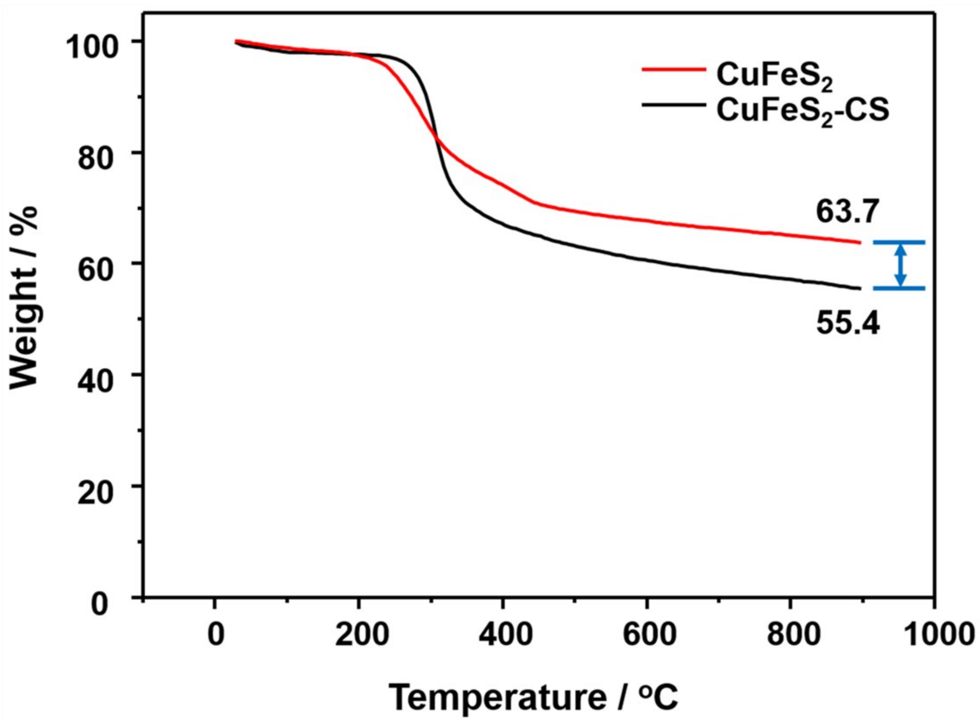

Figure S2. Thermogravimetric analysis (TGA) of a dried sample of $CuFeS_2$ and $CuFeS_2$-CS in the temperature range from room temperature to 800 °C at a heating rate of 10 °C/min in nitrogen.

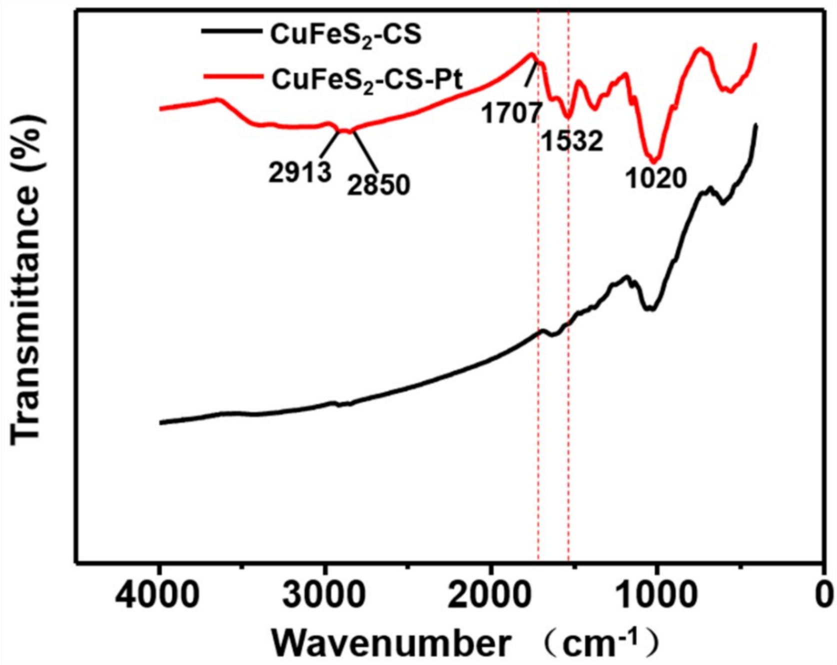

Figure S3. FT-IR spectra of $CuFeS_2$-CS and $CuFeS_2$-CS-Pt, respectively. The -CH_2- strength vibration (2840-2960 cm^{-1}) and -C-C- (1020 cm^{-1}) of CS molecules were observed in the FT-IR. After cis-platinum pro-drug was further attached the $CuFeS_2$-CS NPs, the additional absorption band were observed at 1707 and 1532 cm^{-1}, which was attributed to the C=O, and –NH_2 of amido bond. [1] These observations further confirmed the successful loading of trans-platinum pro-drug to $CuFeS_2$-CS-NPs.

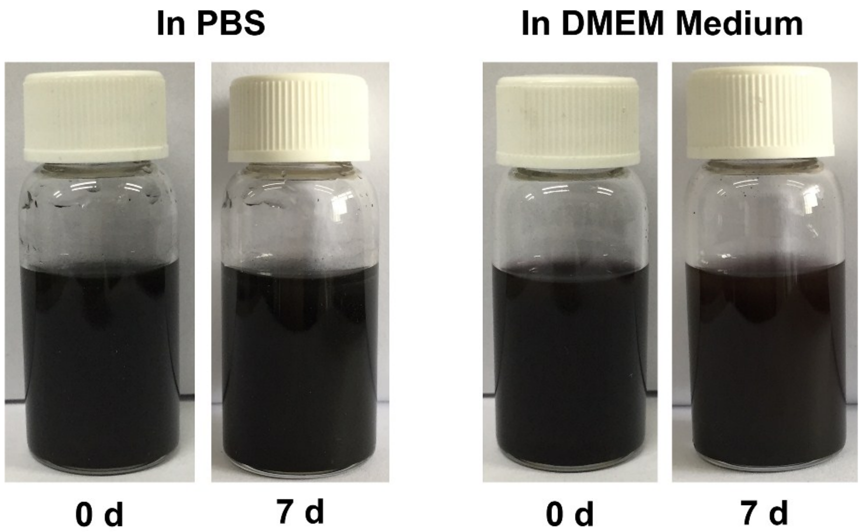

Figure S4. Digital photographs for the dispersion status of $CuFeS_2$-CS dispersed in PBS and DMEM medium at least 7 days, concentration = 1 mM.

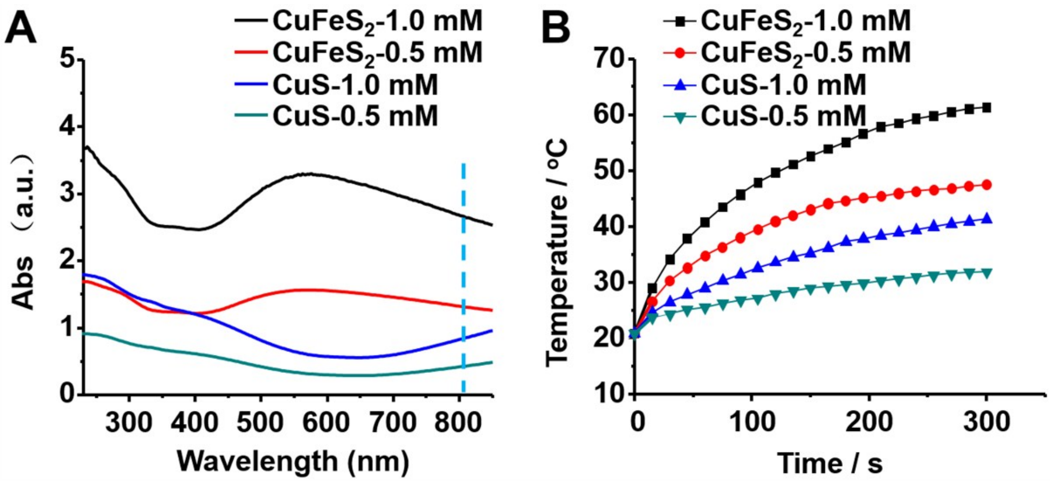

Figure S5. (A) UV-vis-NIR absorption spectra of CuS-CS and $CuFeS_2$-CS dispersed in water at varying Cu^{2+} concentrations (0.5 and 1 mM). (B) Temperature increase of CuS-CS and $CuFeS_2$-CS at varying Cu^{2+} concentrations (0.5 and 1 mM, 200 μL) under laser irradiation (808 nm, 1 W/cm^2) as a function of time (0-300 s).

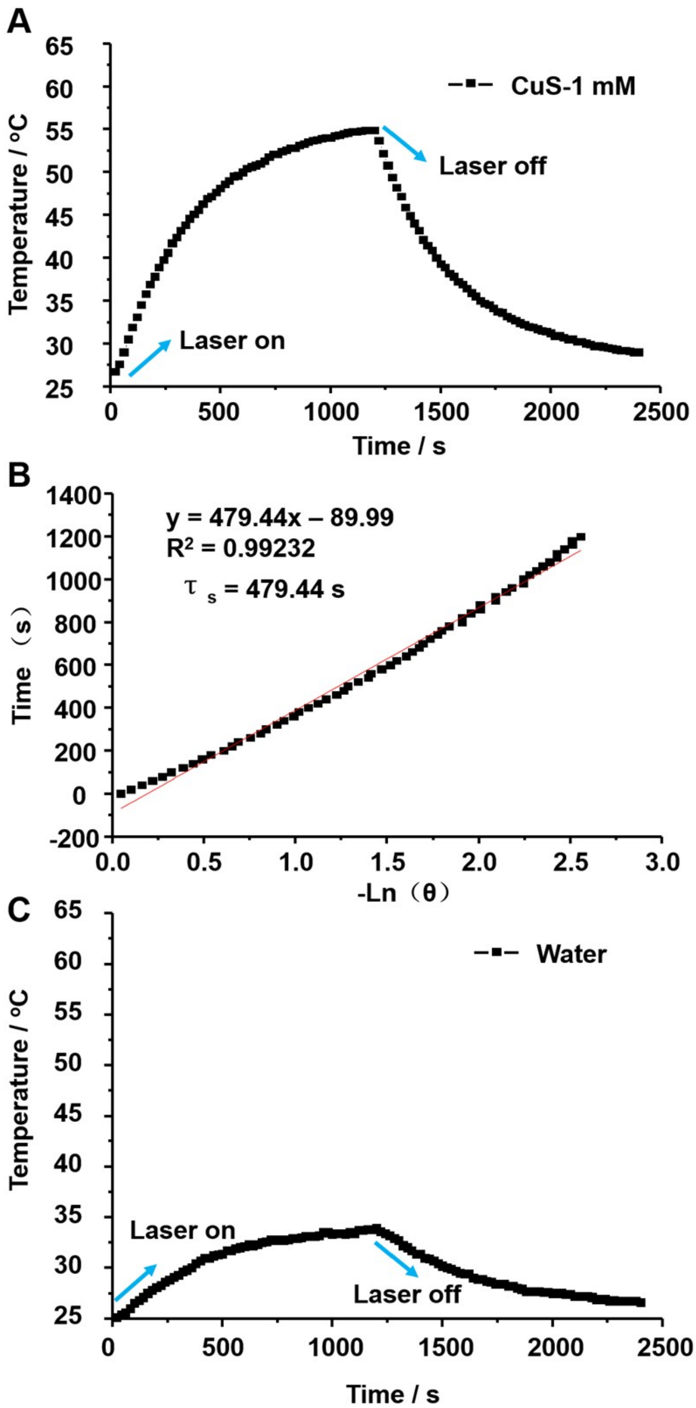

Figure S6. (A) Photothermal effect of a CuS-CS aqueous solution irradiated with a 808 nm laser, and the laser was shut off after irradiation for 20 min. (B) Plot of cooling period (after 20 min) versus negative natural logarithm of driving force temperature. Time constant (τs) for heat transfer from the system is determined to be 479.44 s. (C) Photothermal effect of a pure water irradiated with a 808 nm laser, and the laser was shut off after irradiation for 20 min.

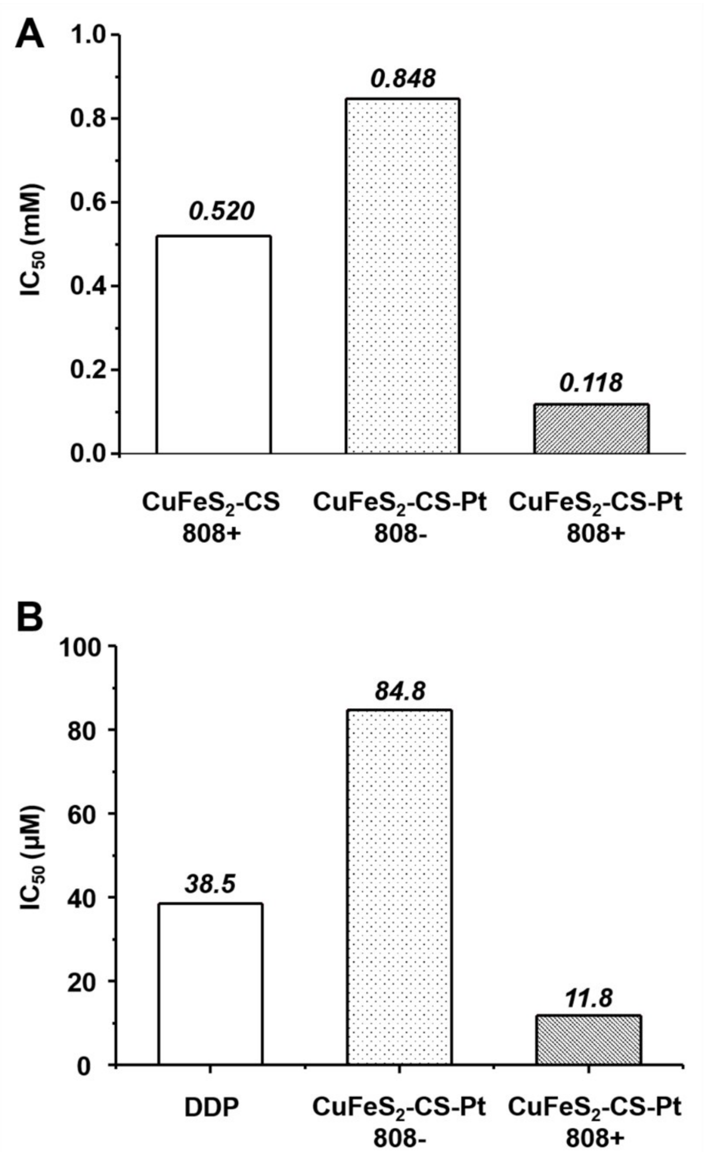

Figure S7. (A) The 50% inhibitory concentration (IC_{50}, Cu) of different treatments: $CuFeS_2$-CS (808+), $CuFeS_2$-CS-Pt (808-) and $CuFeS_2$-CS-Pt (808+). (B) IC_{50} (Pt) of different treatments: DDP, $CuFeS_2$-CS-Pt (808-) and $CuFeS_2$-CS-Pt (808+).

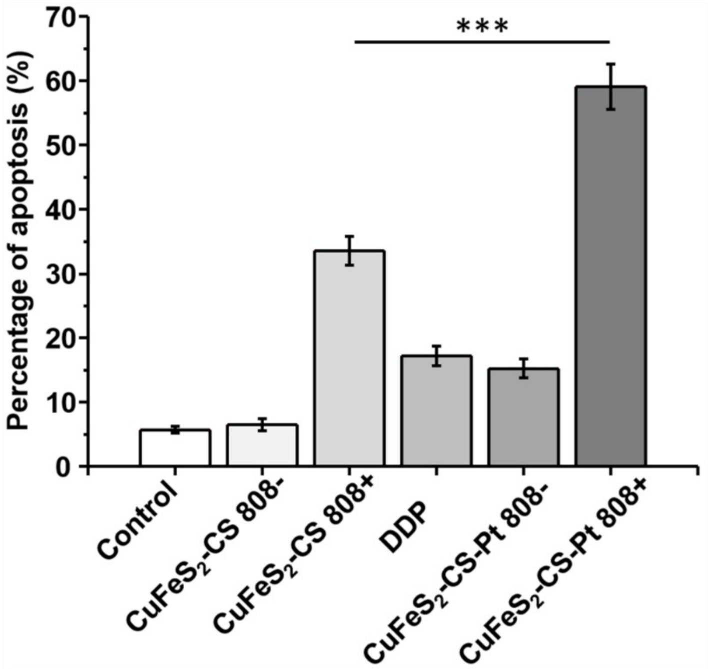

Figure S8. Percentage of apoptosis of A549 cells after different treatments (a) control; (b) $CuFeS_2$-CS (808-); (c) $CuFeS_2$-CS (808+); (d) DDP; (e) $CuFeS_2$-CS-Pt (808-); (f) $CuFeS_2$-CS-Pt (808+). Analysis of Variance (ANOVA) was used to assess statistical significance. *$p< 0.05$, **$p< 0.01$, ***$p< 0.001$.

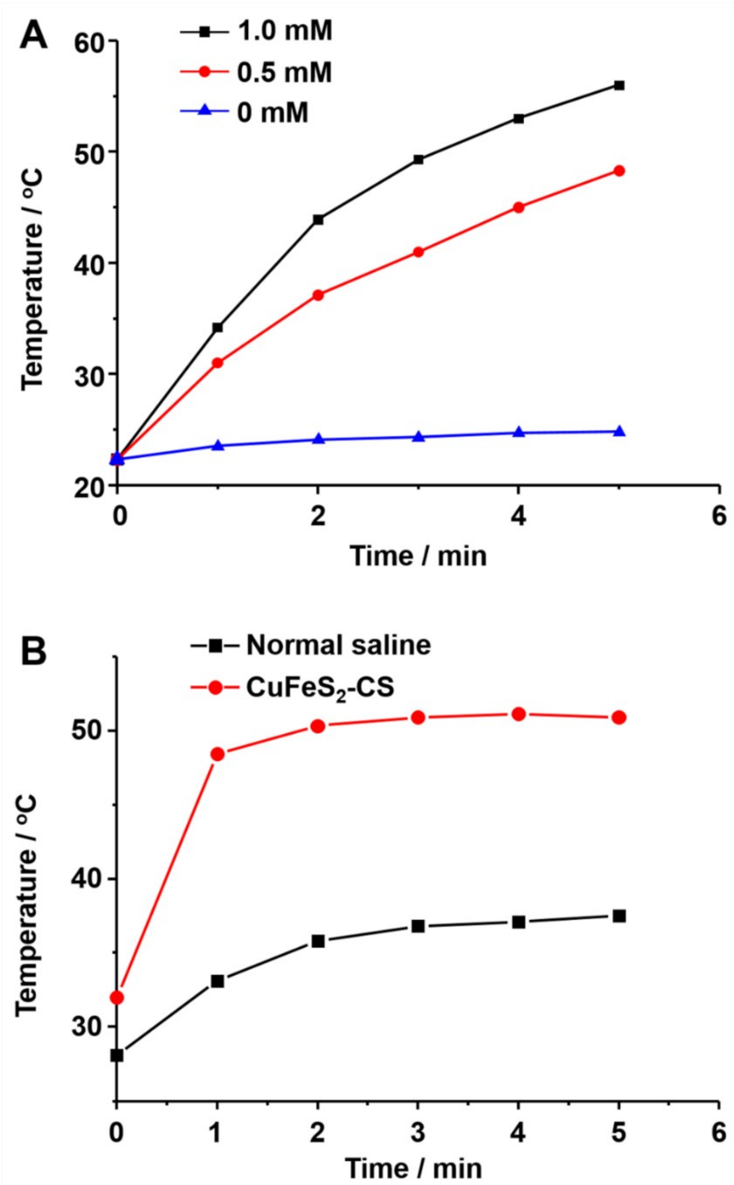

Figure S9. Temperature increase of the vitro thermal imaging of an aqueous $CuFeS_2$-CS solution (2 mL) with different concentrations (A) and A549-tumor-bearing mice with intratumor injection of normal saline and $CuFeS_2$-CS solution (100 μL, 1 mM) (B), exposed to 808 nm laser light (0.5 W/cm^2) for different times (1, 2, 3, 4 and 5 min).

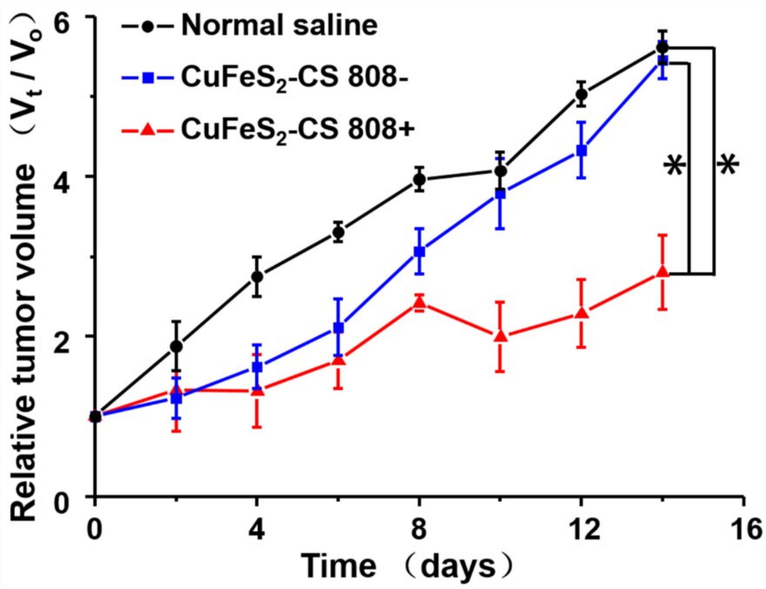

Figure S10. Relative tumor growth curves of H22 tumors after various treatments with normal saline as control; $CuFeS_2$-CS (808-); $CuFeS_2$-CS (808+), respectively. ANOVA was used to assess statistical significance. *p< 0.05, **p< 0.01, ***p< 0.001.

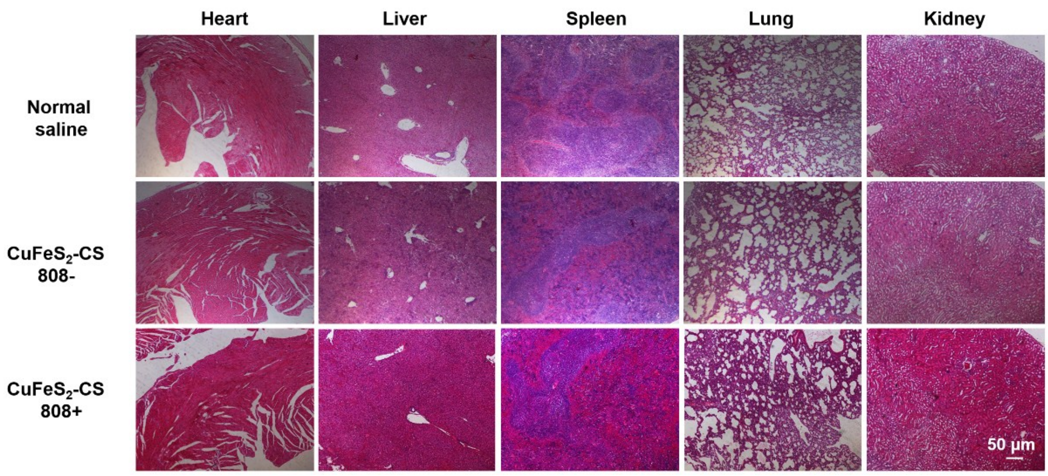

Figure S11. Haematoxylin and eosin (H&E) stained images of major organs of BABL/C mice after various treatments with normal saline as control; $CuFeS_2$-CS (808-); $CuFeS_2$-CS (808+), respectively.

S12. Photothermal conversion efficiency of $CuFeS_2$-CS

To evaluate the photothermal conversion efficiency, a $CuFeS_2$-CS NPs solution (1 mM, 1 mL) was heated to a steady temperature with an 808 nm laser at a power density of 1 W cm^{-2} and then naturally cooled. The photothermal conversion efficiency was calculated according to the previous literature. [2]

$\eta = hS\,(T_{max} - T_{max,water}) / I\,(1-10^{-A})$ (1)

$hS = \Sigma\, m\, Cp/\tau_s$ (2)

$\tau_s = -t/\ln \theta$ (3)

$\theta = (T_{amb}-T)/(T_{amb}-T_{max})$ (4)

where η is the heat transfer coefficient, S is the surface area of container, and T_{max} and $T_{max,\ water}$ are the maximum steady temperatures for $CuFeS_2$-CS NPs solution and water (66.7 and 33.9 ^{o}C, respectively), *I* is the incident laser power density (1 W/cm^2), and A is the absorbance of NPs solution at 808 nm (A = 2.635). m is the mass (1 g) and Cp is the heat capacity [4.2 ×10^3 kJ/(kg • °C)] of water. θ is the dimensionless driving force temperature, T_{amb} is the ambient temperature, and τ_s is the sample system time constant (τ_s= 452.48 s).

Similarly, photothermal conversion efficiency of CuS-CS was calculated. τ_s and η is 479.44 s and 21.4%, respectively.

Table S1. Photothermal conversion efficiency of $CuFeS_2$-CS and CuS-CS.

	Σ m	Cp	τ_s	T_{max} -$T_{max,water}$	*I*	$1-10^{-A}$	η
CuS-CS	1	4.2	479.44	55.0-33.9	1	0.8626	21.4%
$CuFeS_2$-CS	1	4.2	452.48	66.7-33.9	1	0.9977	30.5%

Table S2. Uptake of Pt and the formed Pt-DNA adducts by ICP-MS.

	Time	Pt uptake	Pt-DNA adducts		
			Pt	DNA	Pt/DNA
	min	ng/10^4 cells	pg/10^4 cells	μg/10^4 cells	pg/μg
DDP	10	0.72	1.37	3.27	0.42
		0.83	0.97	4.05	0.24
		0.65	1.48	4.51	0.33
	60	2.45	12.88	4.93	2.61
		1.84	11.23	4.78	2.35
		3.01	13.45	5.21	2.58
$CuFeS_2$-CS-Pt	10	23.53	0.68	3.86	0.18
		20.12	0.82	3.53	0.23
		18.76	0.94	3.31	0.28
	60	68.76	19.75	3.75	5.27
		62.38	16.85	3.52	4.79
		74.26	20.12	4.01	5.02

1. M.-C. Li and U. R. Cho, *Mater. Lett.*, 2013, **92**, 132-135.
2. F. Mao, L. Wen, C. Sun, S. Zhang, G. Wang, J. Zeng, Y. Wang, J. Ma, M. Gao and Z. Li, *ACS Nano*, 2016, **10**, 11145-11155.